Fine Pointing and Tracking Concepts for Optical Intersatellite Links

Eric Miller, Kevin Birnbaum, Chien-Chung Chen, Andrew Grier, Matt Hunwardsen, Dominic Jandrain
Facebook Connectivity
1 Hacker Way, Menlo Park, California, USA

***Abstract*—Free-space optical communication (FSOC) has been promoted for decades as an enabling technology for high-throughput satellite connectivity. However, in order for FSOC to be economically competitive with other technologies (e.g., conventional RF links), the overall manufacturability, including production cost and schedule, needs to be improved.**

One of the major cost and complexity drivers in FSOC systems tends to be the small-space optical assembly associated with fine pointing and tracking. These assemblies typically employ precision optical elements with sensitive alignment requirements, and they sometimes also rely on time-consuming calibration steps which further increase cost and production schedule.

In this paper we present two fine pointing architectures that support high-accuracy pointing, while also featuring simplification of the small-space optical assembly hardware, reduction in the number and complexity of constituent components, full self-calibration capability, and relaxation of otherwise-strict, cost-driving subassembly requirements. One architecture is proposed for short-range applications requiring only limited point-ahead angles, whereas the other architecture supports larger point-ahead angles.

I. Introduction

Free-space optical communication (FSOC) has been promoted for decades as an enabling technology for high-throughput satellite connectivity. However, in order for FSOC to be economically competitive with other technologies (e.g., conventional RF links), the overall manufacturability, including production cost and schedule, needs to be improved.

The highest-throughput FSOC systems make use of coherent detection [1] and/or wavelength-division multiplexing (WDM) [2] – both of which typically involve coupling the receive beam from free space into single-mode optical fiber. Coupling into single-mode fiber also generally enables the use of commercially coherent optical transceiver components, which have seen rapid performance improvements in the last decade, and some of which have even been shown to survive significant exposure to radiation [3].

However, coupling into single-mode fiber requires precision alignment and highly accurate pointing, which can be difficult to achieve even on the ground in a laboratory environment, let alone in the face of time-varying disturbances such as platform motion, vibration, and thermal drift. All of this is made even more complex by the fact that FSOC systems commonly include multiple lines of sight, which can jitter and drift with respect to each other, and which sometimes even need to be pointed separately from each other (e.g., applications requiring non-zero point-ahead).

The conventional solution to this problem is to use some form of closed-loop tracking (e.g., a fast steering mirror and optical track sensor) to reject common-path disturbance, a separate mechanism (e.g., another steering mirror) to apply open-loop point-ahead, and careful opto-mechanical design techniques to minimize launch shift, jitter, and thermal drift effects that would otherwise contribute to misalignment between optical paths [4]. Adjustment mechanisms are also built-in to the hardware design, which skilled engineers and technicians can use to achieve precision alignment during initial assembly.

Unfortunately, this approach tends to drive up hardware complexity in the form of intricate mounting and adjustment features, tight machining tolerances, increased part count, and the use of exotic materials. Furthermore, the manual alignment process can be time-consuming and prone to quality issues, even for skilled engineers and technicians. For systems which require variable point-ahead, the point-ahead mechanism must make use of highly precise and repeatable position sensors, which can further increase cost and may even require their own calibration effort. The end result of this approach is a system that is very complex, and in turn, very expensive to produce.

In this paper, we present two design architectures which make use of a common general idea: employing a single track sensor to simultaneously measure all of the lines of sight in a single system, and then using these co-boresight measurements to enable closed-loop feedback control of the system performance outputs that matter most (i.e., coupling receive light into fiber, and pointing transmit light with respect to receive light). By directly controlling the major performance parameters in closed-loop, we can enable relaxation of otherwise-strict opto-mechanical stability requirements, as well as the reduction in the number of otherwise time-consuming manual alignment and calibration steps – all of which should serve to improve overall production cost and schedule.

II. Detecting multiple spots on a single sensor

Both of the architectures presented herein employ a single track sensor to simultaneously measure multiple lines of sight. There are various ways to accomplish this, and they tend to be analogous to the concepts of spatial-division multiplexing (SDM), time-division multiplexing (TDM), frequency-division multiplexing (FDM), and code-division multiplexing (CDM).

The SDM-like approach generally involves a large-format track sensor, such as a CCD focal plane array, which can

detect multiple laser beam spots, as long as they are spatially separated and resolvable [5], [6]. The downsides of this approach are that large-format sensors tend to be larger, heavier, and more expensive than simpler sensors such as quad cell or lateral effect cell photodiodes. Large-format sensors also are not able to be sampled as quickly, which can limit the achievable closed-loop bandwidth of the jitter rejection mechanism (e.g., FSM). Finally, this approach cannot be used to bring two beams into near-perfect alignment with each other, because the spots must be separated by a certain minimum angular offset in order to be resolvable.

Unlike the SDM approach, the TDM approach can work with beams that are overlapping in space, as long as they are not overlapping in time. The actual time multiplexing mechanism can take the form of repetitive pulsed lasers, which are synchronized and offset in time, or it could consist of discrete communication versus calibration modes with different lasers activated for the different steps. This approach can support the simplest track sensors such as quad cells, enabling improvements in size, weight, power, cost, and sample rate over the SDM approach. However the main downside of this approach is that it does not enable 100 percent operational duty cycle, meaning the data transmission must be stopped sometimes to realign. Furthermore, if the time between realignment sequences is significant, then the system needs to be opto-mechanically stable enough to maintain alignment in-between calibration, which drives back up the hardware complexity and cost of the system.

The last two approaches, FDM and CDM, both involve applying unique modulations to each of the multiple beams (essentially as a carrier signal), and then using the appropriate signal processing approach to demultiplex the individual measurements out of the composite signal. Compared to the previous two approaches, FDM and CDM both enable 100 percent duty cycle operation, both can support fully spatially overlapping beams, and both can be used with simple track sensors such as quad cells or lateral effect cells. And, depending on the details of how the signals are modulated and demodulated, these approaches can also provide additional benefit of background noise rejection in otherwise low-SNR scenarios [7], [8].

The principle behind FDM, synchronous detection, has actually been used for FSOC systems in the past [9]–[11]. However to the best of the current authors' knowledge, these systems all used synchronous detection of only a single tone, for the primary purpose of background noise rejection, rather than for the purpose of multiplexing multiple spots on a single sensor. Here we propose that each of the multiple beams incident on the track sensor would be modulated in amplitude (intensity) with a unique frequency or tone. The composite signal output from the track sensor would then be demodulated multiple ways, producing baseband signals corresponding to each spot.

Code-division multiplexing has also been generally proposed for FSOC systems in the past [8], however the proposed application was essentially for background noise rejection of far-away beacon sources which may not be spatially resolvable from each other. To the best of the authors' knowledge, this paper is the first public mention of using CDM for co-boresight alignment of multiple lines of sight within a single system.

Obviously there are pros and cons to each of the multiplexing approaches mentioned above, but for the remainder of this paper we will focus on FSOC system architectures that could use either FDM or CDM to enable simultaneous line of sight measurements of multiple laser beams on a single track sensor.

III. Two-Tones Fine Pointing Architecture

This architecture uses a single collimator for transmit and receive, a single optical sensor for acquisition and tracking (either a quad cell or lateral effect cell), and a single fast steering mirror (FSM) for precision pointing and jitter rejection. A single dichroic beamsplitter provides high-reflectivity for the outgoing beam, while allowing some amount of the incoming beam to transmit through to the track sensor. Figure 1 illustrates this architecture schematically.

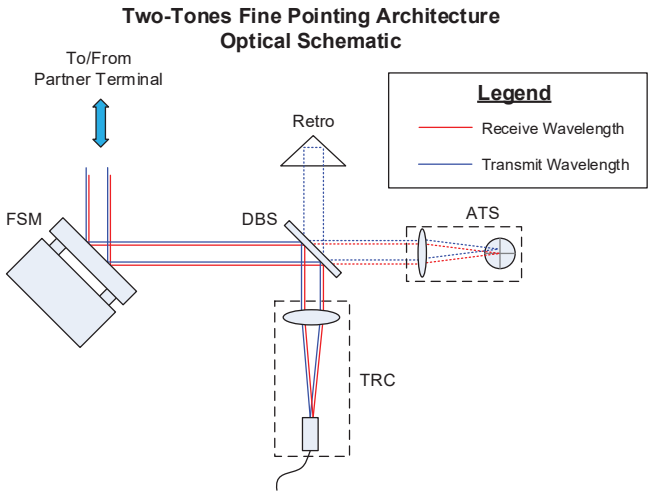

Fig. 1. Optical Schematic, Two-Tones Fine Pointing Architecture (FSM = Fast Steering Mirror, DBS = Dichroic Beam Splitter, ATS = Acquisition & Tracking Sensor, TRC = Transmit/Receive Collimator)

This architecture is not too different from a conventional fine pointing approach, however, the addition of the retro-reflector behind the dichroic beamsplitter enables both incoming and outgoing beams to be detected on the same track sensor. The "two tones" in this architecture's name refer to the incoming and outgoing laser beams, which are each intensity modulated with separate sine tones, so they can be simultaneously detected on the single track sensor.[1] By detecting both beams simultaneously, we can measure and therefore compensate for misalignment and drift between the track sensor and the fiber collimator.

Aside from correcting static misalignments and drift, the simultaneous measurement of incoming and outgoing beams

[1] Although a code-division multiplexing approach as suggested in Section II could be used as well.

on the same track sensor also enables the ability to apply a specified point-ahead angle in optical closed loop. Of course, this architecture has only one collimator and only one FSM, so any point-ahead angle applied by the FSM would result in equal steering for both transmit and receive lines of sight. But rather than apply the entire point-ahead angle to both beams, we could apply half (or some other fraction) of this point-ahead angle, to essentially "split the difference" in pointing loss between transmit and receive links. And since the relationship between pointing error and link loss is exponential, the total link loss due to mis-pointing by half of the point ahead angle on both ends of the link would be less (i.e., better) than the link loss due to mis-pointing by the full point-ahead angle on one end of the link. Applying this concept of "split the difference" point-ahead could enable simple architectures such as the one presented here to support applications which may otherwise require a separate dedicated point-ahead mechanism and collimator, and all of the associated extra complexity and cost.

In the ideal alignment scenario, the retro-reflection from the fiber collimator would show up at the very center of the track sensor, and therefore the two optical paths would be perfectly aligned. However, requiring this to be the case can drive up hardware complexity and cost. So instead, the first thing we do is measure where the light from the collimator shows up on the quad. Next, we add to that position an offset corresponding to the desired amount of point-ahead / look-back. Finally, we use the FSM to steer the incoming laser beam spot to the position on the track sensor corresponding to the sum of the measured collimator spot location, plus the desired look-back offset (which could be zero).

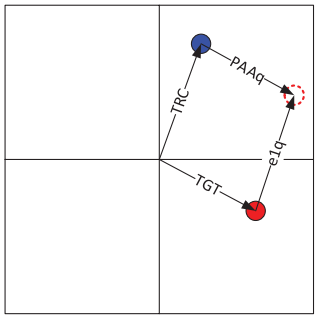

Fig. 2. Track Sensor Spot Illustration, Two-Tones Fine Pointing Architecture. Here, TRC is the location of the spot formed by the beam transmitted by the TX/RX collimator, TGT is the location of the spot formed by the received beam from the target / partner terminal, $PAAq$ represents the desired point-ahead offset between TRC and TGT spots. The FSM works to place the TGT spot on top of TRC spot, thereby driving $e1q$ to zero. (Note that spot sizes in this diagram are not necessarily representative of actual spots formed on the track sensor.)

Figure 2 illustrates the two spots as they land on the track sensor, and shows that the error signal provided to the FSM controller is the difference between the sum of the collimator spot position plus the desired point-ahead offset, minus the position of the incoming spot from the target. In the event that the desired point-ahead is zero, the FSM works to place the incoming target spot directly on top of the collimator spot.

This Two-Tones architecture is simple yet very robust, capable of self-calibration and even able to accommodate small point-ahead angles in closed-loop. For systems requiring larger point-ahead angles, the next architecture will provide even more functionality.

IV. Three-Tones Fine Pointing Architecture

This architecture builds on the previous architecture by incorporating separate transmit and receive collimators (designated as TXC and RXC, respectively), as well as a second FSM (designated as transmit FSM or TFSM, as opposed to the common FSM or CFSM). There are also now two beamsplitters, one to inject the transmit laser into the receive path, and another one to split the receive light between the track sensor and receive collimator. This architecture is illustrated schematically in Figure 3.

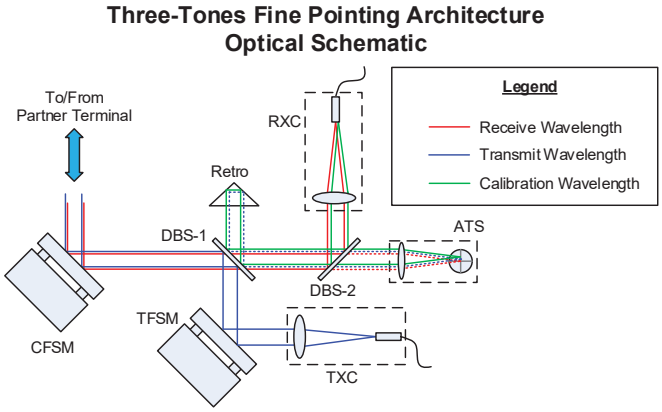

Fig. 3. Optical Schematic, Three-Tones Fine Pointing Architecture. ($CFSM$ = Common Fast Steering Mirror, $TFSM$ = Transmit Fast Steering Mirror, DBS = Dichroic Beam Splitter, RXC = Receive Collimator, TXC = Transmit Beam Splitter, ATS = Acquisition & Tracking Sensor.)

As before, we have a portion of both the incoming laser beam and the outgoing transmit beam focused onto the track sensor. Now that we also have a second collimator, we project a third laser beam out of the receive collimator (made possible by an in-fiber circulator), which is returned off the retro just like the transmit beam, and forms a third spot on the track sensor. And also as before, each of the three beams is modulated with its own unique tone (or code), so they can be separated from the composite signal later in signal processing. (Hence, the "three tones" mentioned in the architecture's name.)

Figure 4 illustrates the three spots as they land on the track sensor. In this diagram, the CFSM works to steer the target spot on top of the RXC spot (making $e1q$ go to zero), and the TFSM works to steer the TXC spot to some specified offset ($PAAq$) with respect to the RXC spot (making $e2q$ go to zero). In the event that no point-ahead offset is desired, the TFSM steers the TXC spot on top of the RXC spot.

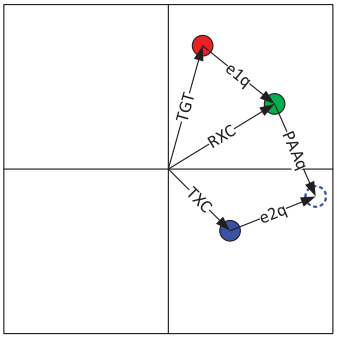

Fig. 4. Track Sensor Spot Illustration, Two Tones Fine Pointing Architecture. Here, RXC represents the location of the spot formed by the laser projected from the receive collimator, TGT represents the location of the spot formed by the laser received from the target / partner terminal, and $e1q$ represents the error term that the $CFSM$ works to drive to zero. TXC represents the location of the spot formed by the laser projected from the transmit collimator, $PAAq$ represents the desired point-ahead offset, and $e2q$ represents the error that the $TFSM$ works to drive to zero.

In summary, the Three Tones fine pointing architecture provides active co-boresight measurement and control, making it capable of self-alignment, and able to apply point-ahead in optical closed-loop. These capabilities should enable the relaxation of otherwise-strict opto-mechanical and FSM requirements, which should help improve the overall system cost and production at scale.

V. Simulation

In this section, we present a demonstration of how the demodulation / demultiplexing approach would work for a scenario representing three separate spots incident on a single detector. Beyond this step, the demultiplexed signals can then be used to control the FSMs as described in Sections III and IV).

For this simulation study, we consider a single detector element, such as a single segment of a quad cell. We first construct three separate baseband signals (a constant, a sine wave, and a square wave), and modulate each of their intensities with a unique carrier tone (at 40, 60, and 90 kHz). Here the baseband signals represent the intensity fluctuations on a single detector element due to misalignment or pointing jitter, and the carrier tones represent the amplitude modulation applied to the beams incident on the detector itself.

We sum these three component signals to form a composite signal, which represents the raw output of the track sensor with three incident spots. The upper plot in Figure 5 shows the "actual" baseband signals, and the lower plot shows the three component signals, each with their carrier tones applied, along with the resulting composite signal. The sample rate in this case was 720 kHz, which all three of the carrier frequencies divide evenly into, and which provides eight samples per cycle of the highest-frequency carrier tone. The formula for the composite signal depicted in Figure 5 is provided in Equation (1).

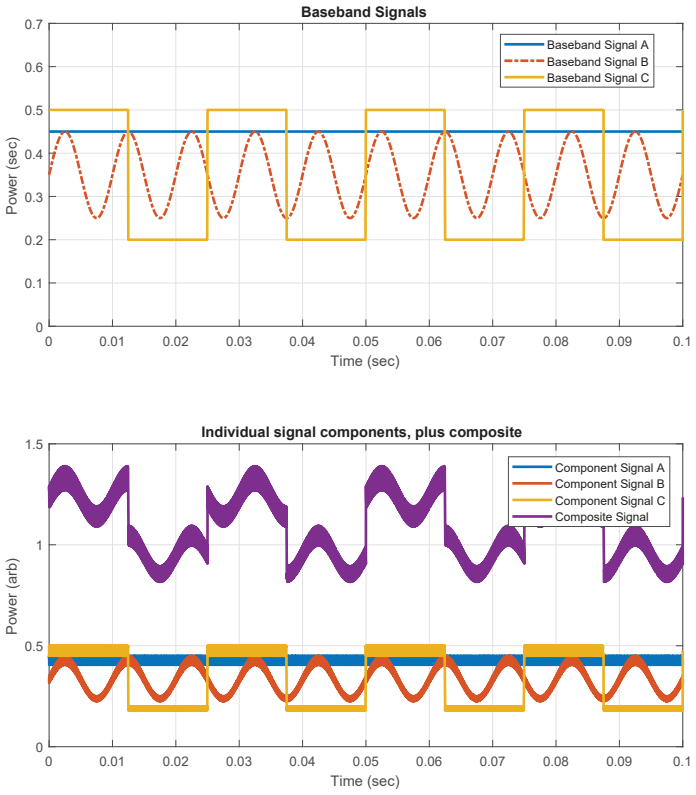

Fig. 5. Upper: Actual Baseband Signals. Lower: Component signals (baseband with carrier modulation), along with composite signal (sum of all three component signals). The parameters used in Equation (1) were $m_a = 0.05$, $f_a = 40e3$ Hz, $m_b = 0.05$, $f_b = 60e3$ Hz, $m_c = 0.05$, $f_c = 90e3$ Hz, $a_a = 0.45$, $a_b = 0.10$, $g_b = 100$ Hz, $w_b = 0.35$, $a_c = 0.15$, $g_c = 40$ Hz, $w_c = 0.35$.

$$
\begin{aligned}
s_{comp,k} &= \big(m_a \sin(2\pi f_a t_k) + (1 - m_a)\big)(a_a) \\
&\quad + \big(m_b \sin(2\pi f_b t_k) + (1 - m_b)\big)(a_b \sin(2\pi g_b t_k) + w_b) \\
&+ \big(m_c \sin(2\pi f_c t_k) + (1 - m_c)\big)\big(a_c \mathrm{sgn}\big(\sin(2\pi g_c t_k)\big) + w_c\big)
\end{aligned} \tag{1}
$$

The next step is to generate reference sinusoids for each of the three carriers, and then mix the composite signal with each of these reference sines to shift the desired baseband signals down to DC. Figure 6 shows the frequency spectrum of the composite signal (top plot), along with the spectra of the composite signal after mixing with each of the three reference tones. As evident in the lower three plots, these mixed products include a reconstruction of the original baseband signals back near DC, but they also shift the other components up and down by the frequency of the reference sine. For example, when the composite signal is mixed with the reference sine at 40 kHz, the 40 kHz component of the composite signal moves down to DC (and up to 80 kHz), but also the DC component of the composite signal moves up to 40 kHz, the 60 kHz component moves down to 20 kHz, and the 90 kHz signal shifts down to 50 kHz. These new components at 20, 40, and 50 kHz

represent interference or noise on the reconstruction of the intended baseband signal.

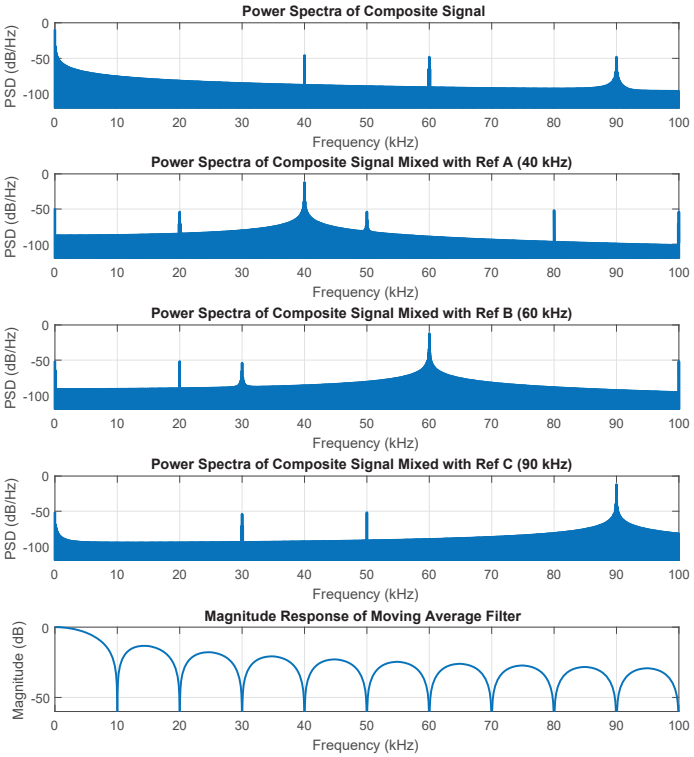

Fig. 6. Power Spectra of composite signal (top), power spectra of composite mixed with the three reference sines (middle three), and frequency response of 72-point moving average filter (bottom). Parameters used here were the same as defined in Figure 5.

One way to evaluate the viability of this approach would be to compare the reconstructions against the actual baseband signals. However, this comparison would reveal that the reconstruction signals have a significant amount of high-frequency noise, due to the interference terms mentioned above. Fortunately, in the context of the two fine pointing architectures presented above, these reconstructed signals are subsequently filtered by the mechanical transfer function of the fast steering mirror, which acts as a low-pass filter. So instead, we look at the comparison between the FSM response to the actual baseband, versus the FSM response to the reconstructed baseband. For this comparison, we use a notional FSM closed-loop transfer function with a -3dB crossover at 1,000 Hz. Figure 7 shows the FSM transfer function, and Figure 8 shows the resulting FSM responses to the actual baseband versus reconstructed baseband.

Upon inspection of the curves in Figure 8, one may notice that even after being filtered by the FSM mechanical response, the resulting signal still exhibits a significant amount of high-frequency noise. Further investigation would reveal that this high-frequency noise is at the same frequency as the interference terms described above. In an attempt to clean up this signal, we also simulated the case where the reconstructed baseband signal is filtered by a moving average filter before going to the FSM. In this scenario, the filter consisted of a

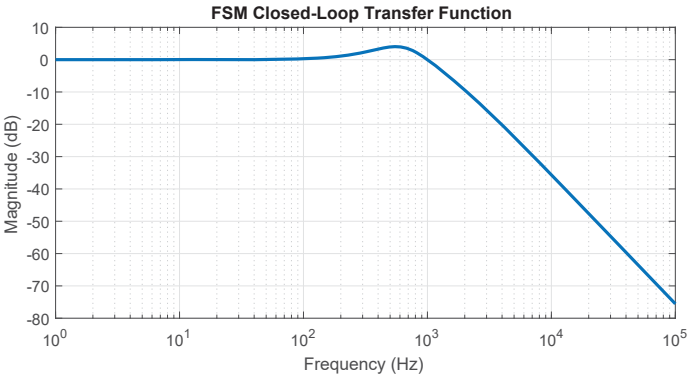

Fig. 7. FSM transfer function

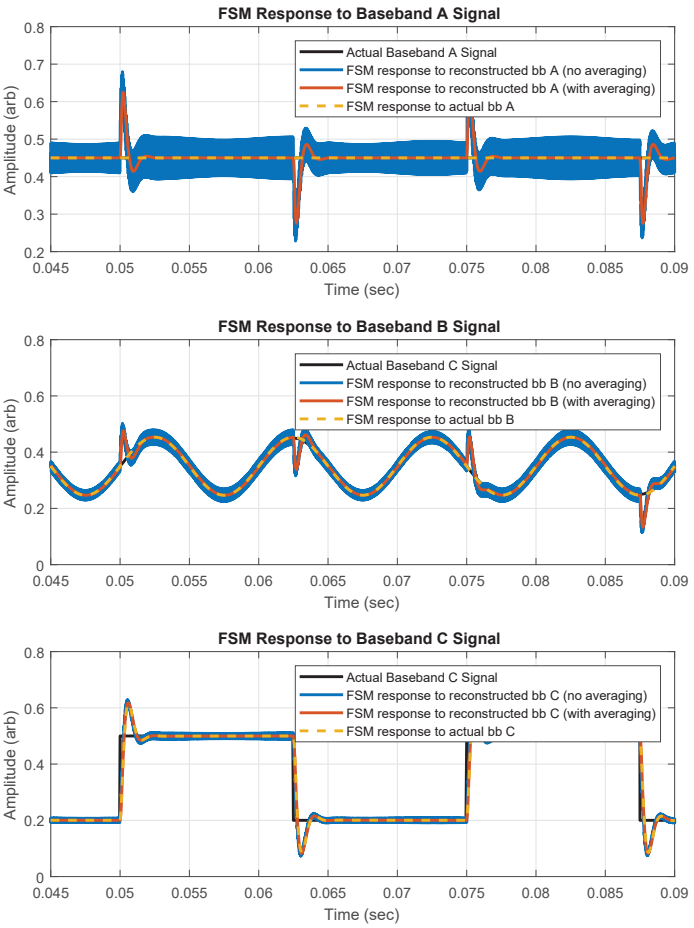

Fig. 8. FSM response to actual versus reconstructed baseband signals. Parameters used here were the same as defined in Figure 5.

simple moving average of the last 72 samples, which was carefully selected to ensure that, over the sample period of the averaging filter, the various carrier tones would be orthogonal, and therefore the filtered version of the reconstructed baseband signals would exhibit nearly zero effects of the interference terms mentioned above. (This is similar to what was done in [12] with two tones.) The magnitude plot of the averaging filter is shown in Figure 6. Looking at Figure 8, the FSM

responses to the moving-average filtered baseband signals exhibit nearly none of the high-frequency noise apparent on the FSM response to the non-filtered baseband signals.

One other interesting feature visible on Figure 8 is the fact that there is some cross-talk from the third baseband signal (a square wave) showing up on the other two reconstructions. Figure 9 provides a zoomed-in view of this effect using the same data as Figure 8. In reality, a perfect square wave is an unlikely disturbance to arise from physical phenomena – however, the notion of crosstalk, especially due to higher-frequency signal features, may be worthy of further investigation.

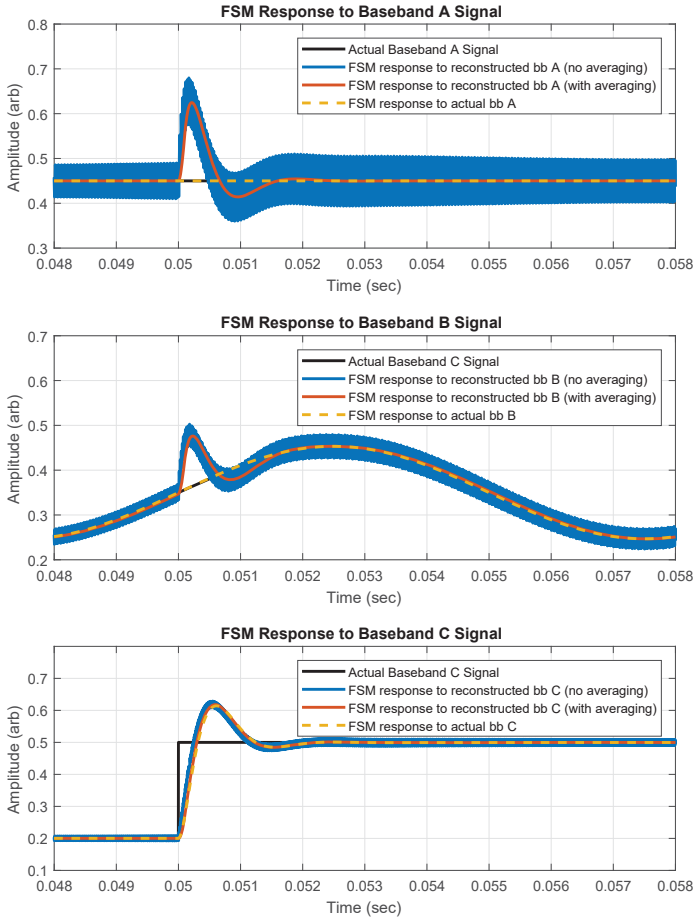

Fig. 9. FSM response to actual versus reconstructed baseband signals. Parameters used here were the same as defined in Figure 5.

VI. Conclusion

This paper presented two fine pointing architectures for free-space laser communication systems, both of which use the general concept of simultaneous measurement of multiple laser beams on a single detector to enable automatic self-alignment and closed-loop point-ahead control. This concept of simultaneously detecting multiple signals via frequency-division multiplexing was also demonstrated via simulation. The enhanced capabilities of these architectures should enable detailed opto-mechanical design to proceed with relaxed requirements compared to a "conventional" approach, leading to reductions in complexity, cost, and manufacturability at scale.

In the future, we believe that a more-detailed study of the pros and cons between frequency-division, code-division, and even time-division multiplexing, in the context of active co-boresight measurement and control would make for an interesting research topic. Also, an investigation into alternative digital filter formulations that maximize interference rejection while minimizing phase loss of the desired signal (other than the moving average filter simulated above) would be interesting as well.

Ultimately, we hope that the fine pointing architectures described herein will be used to develop low-cost, easily manufacturable FSOC systems, which will help enhance satellite connectivity networks and bring internet to the entire world.

Acknowledgment

The authors would like to thank Bart McGuyer, Harvard Harding, Chiyun Xia, and Hamid Hemmati for their thoughtful review and advice.

References

[1] C. Chen, A. Grier, M. Malfa, E. Booen, H. Harding, C. Xia, M. Hunwardsen, J. Demers, K. Kudinov, G. Mak, B. Smith, A. Sahasrabudhe, F. Patawaran, T. Wang, A. Wang, C. Zhao, D. Leang, J. Gin, M. Lewis, D. Nguyen, and K. Quirk, "High-speed optical links for UAV applications," *Proc. of SPIE*, vol. 10096, 2017.

[2] D. Giggenbach, J. Poliak, R. Mata-Calvo, C. Fuchs, N. Perlot, R. Freund, and T. Richter, "Preliminary results of Terabit-per-second long-range free-space optical transmission Experiment THRUST," *Proc. of SPIE*, vol. 9647-21, 2015.

[3] R. Aniceto, S. Moro, R. Milanowski, C. Isabelle, N. Hall, and K. Cahoy, "Single Event Effect and Total Ionizing Dose Assessment of Commercial Optical Coherent DSP ASIC," *Presented at NSREC 2017 Radiation Effects Data Workshop*, 2017. [Online]. Available: https://research.fb.com/publications/coherent-asic-see-tid-testing/

[4] H. Hemmati, *Near-Earth Laser Communications*, 2009.

[5] D. L. Clark, M. Cosgrove, R. VanVranken, H. Park, and M. Fitzmaurice, "Application of single area array detector for ATP in space optical communications," *Proc. of SPIE*, vol. 1044, 1989.

[6] D. Russell, H. Ansari, and C.-c. Chen, "LaserCom Pointing Acquisition and Tracking Control," *Proc. of SPIE Vol. 2123*, 1994.

[7] D. P. Blair and P. H. Sydenham, "Phase sensitive detection as a means to recover signals buried in noise," *Journal of Physics E: Scientific Instruments*, vol. 8, 1975.

[8] K. M. Birnbaum, A. Sahasrabudhe, and W. H. Farr, "Separating and tracking multiple beacon sources for deep space optical communications," *Proc. of SPIE*, vol. 7587, 2010.

[9] D. Greenwald and C. Mclaughlin, "A beacon tracker and point ahead system for optical communications," *Proc. of SPIE*, vol. 1111, 1989.

[10] P. V. LaSala and C. McLaughlin, "Beam tracker and point ahead system for optical communications II - servo performance," *Proc. of SPIE*, vol. 1482, 1991.

[11] W. Hayden, T. McCullough, A. Reth, and D. Kaufman, "Wide-band precision two-axis beam steerer tracking servo design and," *Proc. of SPIE*, vol. 1866, 1993.

[12] J. M. Masciotti, J. M. Lasker, and A. H. Hielscher, "Digital lock-in detection for discriminating multiple modulation frequencies with high accuracy and computational efficiency," *IEEE Transactions on Instrumentation and Measurement*, vol. 57, no. 1, 2008.